JOC The Journal of Organic Chemistry

Article

pubs.acs.org/joc

Theoretical Study on the Mechanism of Stereoselective Synthesis of Oxazolidinones

Abing Duan, Liang Peng, Daoling Peng, and Feng Long Gu*

Key Laboratory of Theoretical Chemistry of Environment, Ministry of Education, School of Chemistry and Environment, South China Normal University, Guangzhou 510006, China

Supporting Information

ABSTRACT: Oxazolidinones can be synthesized through an organocatalytic cascade reaction of stable sulfur ylides and nitro-olefins. This process, sequentially catalyzed by thiourea and *N*,*N*-dimethylaminopyridine (DMAP), is theoretically studied using density functional theory by the continuum solvation model. It is shown that the rate- and stereoselectivity-determining step is the addition reaction of sulfur ylide to the nitro-olefin with two competing reaction channels. One channel is where the nitro-cyclopropane is generated first and then converted into isoxazoline *N*-oxide through a DMAP-catalyzed rearrangement. The other channel is the direct generation of the isoxazoline *N*-oxide intermediate. DMAP plays an important role in the reaction as a nucleophilic catalyst. The mechanism for the important rearrangement reaction proposed by Xiao et al. (*J. Am. Chem. Soc.* **2008**, *130*, 6946−6948) is not appropriate as the reaction energy barrier is too high; a 10-step mechanism determined by our theoretical calculations is more feasible as the energy barrier is becoming much less than that by Xiao. It is the first time that the Hofmann rearrangement involved in the cascade organocatalysis is confirmed by theoretical calculations. Our result of the stereoselectivity for the synthesis of oxazolidinones is in good agreement with the experiment.

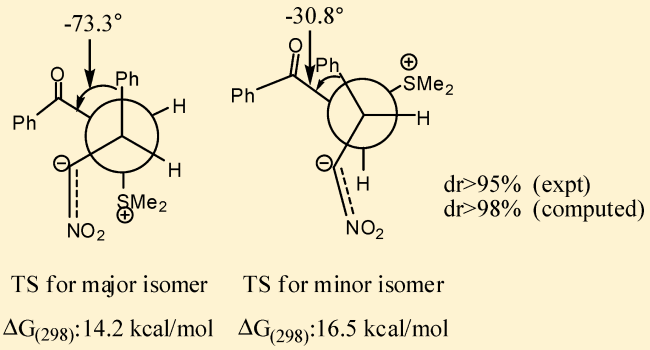

INTRODUCTION

Oxazolidinone and its derivatives are not only biologically active heterocyclic compounds[1] but also important intermediates in organic synthesis. They are often used as chiral auxiliaries,[2−4] catalysts, and ligands, with wide applications in biology, medicine, and chemistry.[5−9] Moreover, oxazolidinone and derivative chiral amino alcohol are basic units of many natural products. For example, cytoxazone, isolated from Streptomyces by the Osada group[10] in 1998, is a novel cytokine modulator which interferes with the cytokine IL-4, IL-10, and IgG produced by selective inhibition of the signaling pathway of Th2 cells. In addition, taxol side chain and Valinotin A contain an α-amino-β-hydroxy acid fragment, which is derived from oxazolidinone.[11,12]

Xiao et al.[13] recently developed a new method to synthesize oxazolidinone through cascade organocatalysis. In his method, stable sulfur ylides and nitro-olefins catalyzed by thiourea together with *N*,*N*-dimethylaminopyridine (DMAP) (see Figure 1 for details) were used to produce oxazolidinone, and

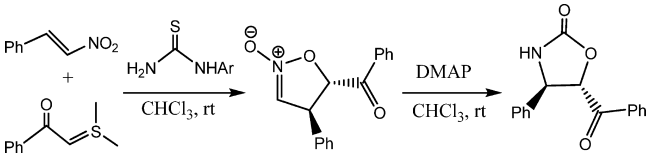

Figure 1. Organocatalyzed cascade reaction of sulfur ylide with nitro-olefins.

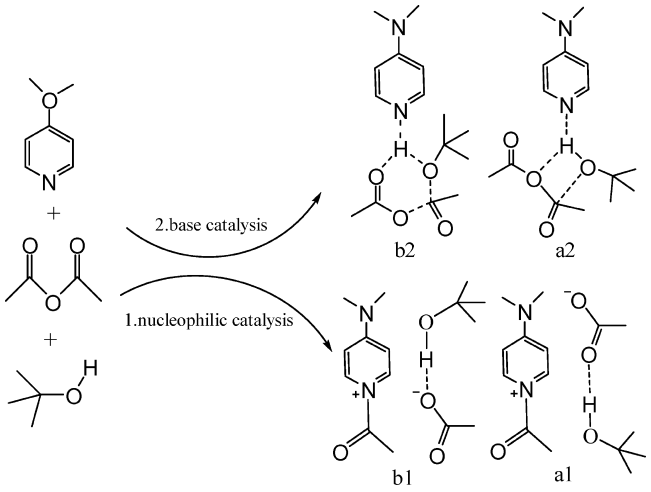

Figure 2. Competing nucleophilic and base catalysis mechanisms in the DMAP-catalyzed reaction of acetic anhydride with *tert*-butyl alcohol.

Received: October 8, 2013
Published: November 15, 2013

   dx.doi.org/10.1021/jo4022452 | J. Org. Chem. 2013, 78, 12585−12592

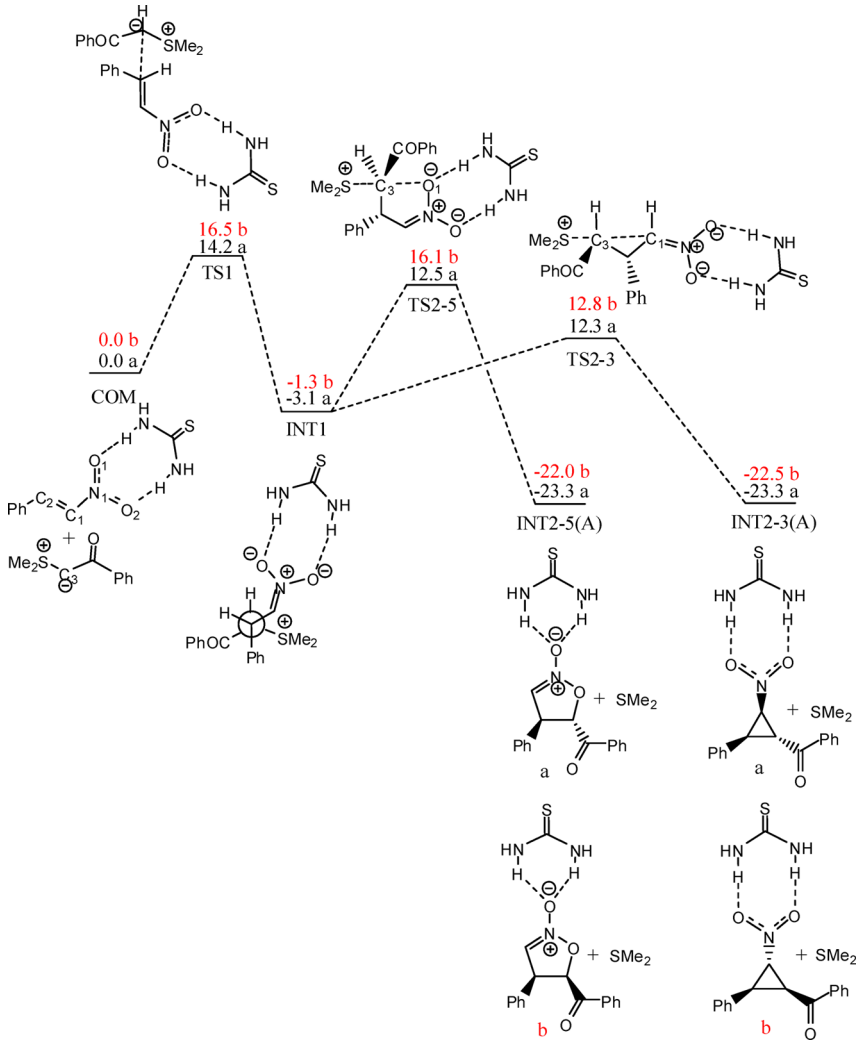

Figure 3. relative free energies (ΔG_{298}) (in kcal/mol) of acid-catalyzed process at the M06-2X/6-31G (d,p) level: (a) trans configuration, (b) cis configuration. The trans and cis vary depend on the positions of Ph and PhCO at the INT2-3(A) or INT2-5(A). Only the trans structure is presented here, except for INT2-3(A) and INT2-5(A).

the reaction afforded the products with high yields and great diastereoselectivity (dr >95:5). Further studies[14,15] by Xiao's group were carried out by using different sulfur ylides and solvent. A good reaction condition was obtained to provide high diastereoselectivity (dr >95:5) and high enantioselectivity (er 95:5).

DMAP is believed to be one of the most useful nucleophilic catalysts, especially for catalyzing the acylation of alcohols.[16] The mechanism of the DMAP-catalyzed acetylation of alcohols is extensively studied both experimentally and theoretically.[17,18] It is considered that there are two competitive pathways, that is, the base-catalyzed pathway and the nucleophilic attack pathway, as illustrated in Figure 2. A theoretical study by Xu et al.[17] shows that the latter is more favorable in the acylation reaction of alcohols catalyzed by anhydrides and acyl chlorides. Therefore, the nucleophilic effect of DMAP should be taken into account in the study of the isomerization reaction of nitrogen oxides on isoxazoline.

Recently, Wheeler et al.[19] used density functional theory (DFT) to study the stereoselectivities of transition states with different π-stacking interactions. It has be shown by Krenske et al.[20] that aromatic interactions (π-stacking, CH$-\pi$, cation$-\pi$, and anion$-\pi$ interactions) control the stereoselectivities of organic reactions, and the dr value evaluated by the M06-2X[21] functional is very close to the experimental result. In this work, we use DFT with the M06-2X functional to investigate the mechanism of stereoselective synthesis of oxazolidinones, to further understand the mechanism by theoretical calculations. Our study is to find the origin of selectivity and high yield of such kinds of reactions.

■ COMPUTATIONAL DETAILS

The M06-2X exchange-correlation functional developed by Zhao and Truhlar[22] has been shown to provide a better description for noncovalent interactions than the conventional density functionals. Zhao et al.[22−24] recommend the M06-2X functional for applications involving main-group thermochemistry, kinetics, noncovalent interactions, and electronic excitation energies to valence and Rydberg states. Optimized stationary points (reactant and transition structure geometries) were characterized by vibrational frequency calculations at the M06-2X[22−24]/6-31G(d,p) level in the presence of the continuum solvation model[26] (SMD) with chloroform (ε = 4.71, R_{solv} = 2.48 Å) as solvent. One can find the results at the B3LYP[25]/6-31G(d,p) level in the Supporting Information. The basis set effects have been investigated, as shown in Table 1. It is found that the size of the basis sets does not significantly affect the electronic energies, especially for the transition states. From Table 1, one can see that the 6-31G(d,p) basis set is appropriate to describe the system since larger basis sets do

dx.doi.org/10.1021/jo4022452 | J. Org. Chem. 2013, 78, 12585−12592

Table 1. Energy (in kcal/mol) of Various Structures with Different Basis Sets in the Acid-Catalyzed Process Stereoselectivity and Transition States

basis set	structure	Δ(E+ZPE)	ΔG	ΔH
		M06-2X		
6-31G(d,p)	com	0.0	0.0	0.0
	TS1-trans	13.1	14.2	12.4
	TS1-cis	15.1	16.5	14.3
	TS2-trans	11.7	12.5	10.9
	TS2-rrr	11.7	12.3	11.0
6-31+G(d,p)	com	0.0	0.0	0.0
	TS1-trans	12.2	14.8	11.3
	TS1-cis	13.5	15.2	12.8
	TS2-trans	10.6	12.5	9.6
	TS2-rrr	11.3	12.4	10.6
6-31++G(d,p)	com	0.0	0.0	0.0
	TS1-trans	12.1	14.0	11.3
	TS1-cis	13.3	14.7	12.6
	TS2-trans	10.6	12.1	9.6
	TS2-rrr	11.2	11.9	10.6
6-311G(d,p)	com	0.0	0.0	0.0
	TS1-trans	12.9	16.3	12.0
	TS1-cis	14.8	17.0	14.0
	TS2-trans	13.1	16.0	11.9
	TS2-rrr	13.1	14.7	12.3
6-311++G(d,p)	com	0.0	0.0	0.0
	TS1-trans	12.0	13.6	11.4
	TS1-cis	13.5	14.6	12.9
	TS2-trans	10.8	12.3	9.9
	TS2-rrr	11.8	12.2	11.3

Table 2. Relative Free Energies (in kcal/mol) of Stable Points in the Acid-Catalyzed Process (a, trans configuration; b, cis configuration)

structure	Δ(E+ZPE)	ΔG	ΔH	Δ(E+ZPE)	ΔG	ΔH
	M06-2X/6-31G(d,p) (without thiourea)			M06-2X/6-31G(d,p) (with thiourea)		
com	0.0	0.0	0.0	0.0	0.0	0.0
TS1-a	12.2	17.4	10.8	13.1	14.2	12.4
TS1-b	12.4	17.0	11.1	15.1	16.5	14.3
INT1-a	−1.2	3.9	−2.6	−3.5	−3.1	−4.5
INT1-b	0.7	5.5	−0.6	−1.7	−1.3	−2.6
TS2-5a	12.1	16.6	10.8	11.7	12.5	10.9
TS2-5b	14.3	20.1	12.7	14.2	16.1	13.2
INT2-5a(A)	−29.3	−26.8	−30.1	−21.0	−23.3	−21.0
INT2-5b(A)	−24.6	−22.6	−25.4	−20.4	−22.0	−20.7
TS2-3a	9.8	13.4	8.7	11.7	12.3	11.0
TS2-3b	11.2	15.2	10.1	13.2	12.8	12.6
INT2-3a(A)	−28.9	−28.0	−29.3	−20.9	−23.3	−20.9
INT2-3b(A)	−31.2	−28.4	−31.9	−19.7	−22.5	−19.2

not significantly improve the result. For the largest basis set, 6-311++G(d,p) compared to 6-31G(d,p) for different structure, one can find that ΔΔG is −0.6, −1.9, −0.2, and −0.1, respectively, for TS1-trans, TS1-cis, TS2-trans, and TS2-rrr. In order to save computing resources, only the 6-31G(d,p) basis set is employed for the following studies. There are many isomers with different conformations in stationary points, and only the most stable one was considered. TS1, TS3, and TS10 are confirmed by IRC calculations and the others by analysis of the vectors associated with imaginary frequency. The vibrational frequency calculations were performed in order to obtain thermodynamic data at 298 K and were also used to verify whether the structure is a true stationary point. All computations were performed using the Gaussian09 program.[27]

Table 3. Relative Free Energies (in kcal/mol) of Stable Points in Converting INT2-3(B) to INT2-5(B)

structure	Δ(E+ZPE)	ΔG	ΔH
		M06-2X/6-31G(d,p)	
INT2-3(B)	0.0	0.0	0.0
TS2-c1	33.9	36.4	33.6
INT2-c	4.4	7.9	3.8
TS2-c2	29.4	32.5	28.9
INT2-5(B)	2.9	5.4	2.9

Table 4. Relative Free Energies (in kcal/mol) of Isoxazoline *N*-Oxide 6 and Oxaziridine 7 Suggested by Experimentalists

structure	Δ(E+ZPE)	ΔG	ΔH
6	0.0	0.0	0.0
TS(6-7)	52.3	53.7	52.0
7	10.3	9.5	10.2

Table 5. Relative Free Energies (in kcal/mol) of Stable Points of Rearrangement Reaction in the Base-Catalyzed Process

structure	Δ(E+ZPE)	ΔG	ΔH
		M06-2X/6-31G(d,p)	
INT2-5(B)	0.0	0.0	0.0
TS3	18.4	21.2	17.3
INT3	−1.6	−1.0	−1.9
TS4	3.0	4.3	2.5
INT4	−24.7	−22.7	−25.4
TS5	−12.5	−11.0	−13.3
INT5	−19.8	−17.7	−20.6
TS6	−1.5	0.3	−2.4
INT6	−4.4	−2.5	−5.2
TS7	0.5	2.7	−0.3
INT7	−24.9	−25.1	−25.1
TS8	−1.2	−2.3	−1.1
INT8	−28.0	−27.1	−28.3
TS9	−0.8	0.6	−1.3
INT9	−15.3	−16.9	−15.3
TS10	8.3	8.8	8.4
INT10	−77.3	−77.7	−76.9
TS11	−73.4	−73.6	−73.5
INT11	−89.1	−90.0	−89.4
TS12	−90.5	−90.9	−91.0
P	−95.0	−94.6	−95.3

RESULTS AND DISCUSSION

Acid Catalysis Process. As inferred by Xiao et al.,[13] the acid catalysis process includes two steps, and the process is depicted in Figure 3. The first step is an addition reaction where the nitro-olefin is activated by the thiourea catalysis through two hydrogen bonds and followed by the addition of sulfur ylide to nitro-olefin to form nitronate. The formed nitronate is stabilized by hydrogen bonds between the nitronate group and thiourea. The free energy barriers of the transition state have been calculated by M06-2X/6-31G(d,p) with the SMD solvent model. The results are listed in Table 2. From Table 2, one can see that the free energy barriers are 14.2 kcal/mol for trans configuration and 16.5 kcal/mol for cis configuration. Therefore, the trans configuration is more stable, and it should be the predominant form.

dx.doi.org/10.1021/jo4022452 | J. Org. Chem. 2013, 78, 12585−12592

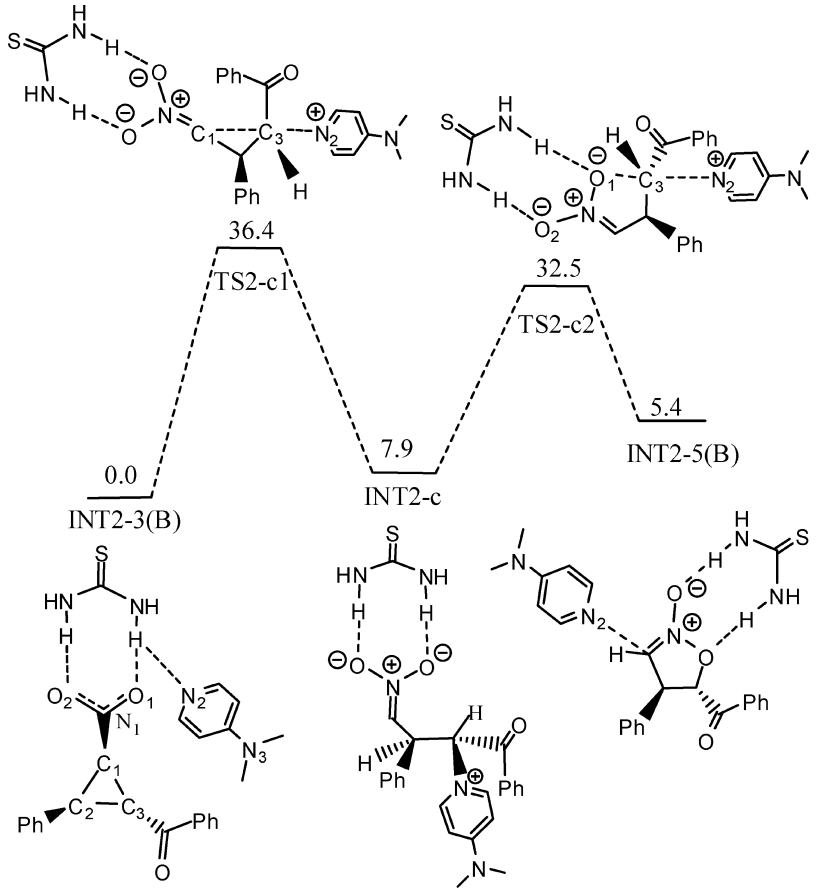

Figure 4. Relative free energies (ΔG_{298}) (in kcal/mol) of INT2-3(B) to INT2-5(B) trans configuration in the base-catalyzed process with SMD solvent models at the M06-2X/6-31G(d,p) level.

The second step is an intramolecular substitution reaction. There exist two competitive reaction pathways: (1) As suggested by Xiao et al.,[13] atom O1 of the nitro group attacks C3 and then affords the oxazoline *N*-oxide (INT2-5(A)). (2) C1 attacks C3 to form a cyclopropane (INT2-3(A)). The leaving group is sulfide for both reaction pathways. M06-2X calculations indicate that the trans configuration of two reaction paths is competitive, while for the cis configuration, the second reaction path is dominant. The relative energies to the reactant complex are 12.5 and 12.3 kcal/mol for trans and 16.1 and 12.8 kcal/mol for cis configuration. From our calculations, whether a three-membered ring or a five-membered ring is generated, the trans configuration pathway is the favorite reaction path. This is in good agreement with the experiment observation.

From Table 2, one can know that thiourea in the acid catalysis process plays a very important role. Without thiourea, the free energy barriers of the transition state for the first step is 17.4 kcal/mol for the trans configuration and 17.0 kcal/mol for the cis configuration, and the cis configuration is the predominant form, with the value of dr being 66%. The free energy barriers with thiourea are, respectively, decreased to 14.2 and 16.5 kcal/mol; therefore, the trans configuration is the predominant form, and the value of dr is 98%. What's more, the free energy barriers for other structures (except for INT1-a and INT1-b) with thiourea in the acid-catalyzed process are all lower than those of the system without thiourea. So, thiourea plays an important role not only decreasing the energy barrier but also improving the diastereoselectivity.

The first step is the rate-determining step of the reaction process regardless of the configuration of intermediates. Our results of M06-2X show that INT2-3(A) and INT2-5(A) are competitive, while the results of B3LYP show that the INT2-3(A) configuration is the major product of the acid-catalyzed process and the intermediate INT2-5(A) can be detected in the course of the experiment, which is in agreement with the experimental results. One can argue that INT2-3(A) can be transformed to INT2-5(A) under the experimental conditions. For this purpose, a pathway where INT2-3(A) is converted to INT2-5(A) is designed, and it will be discussed in the next section of the base-catalyzed process.

Base Catalysis Process. the theoretical study of Xu et al.[17] shows that the nucleophilic catalytic reaction is a favorable reaction pathway in the acylation reaction of the alcohol with acid anhydride or chloride. DMAP plays an important role during the nucleophilic catalysis mechanism because it will have an intermediate with the acetylpyridinium of DMAP. In the base catalysis process, one should consider the role of the DMAP as a nucleophilic catalyst.

Therefore, a two-step nucleophilic substitution reaction catalyzed by DMAP is designed for the conversion from INT2-3(B) to INT2-5(B) (Figure 4). The first step is that the N2 of DMAP attacks the C3 and breaks the C1−C3 bond. The configuration of C3 is inversed at this step. The second step is that the O1 of NO_2 attacks the C3 to form INT2-5(B). DMAP is regenerated, and the configuration of C3 is inversed again. Since the inversion happens twice, the configuration of C3 does not change after these two attacks. The results of M06-2X are presented in

dx.doi.org/10.1021/jo4022452 | J. Org. Chem. 2013, 78, 12585−12592

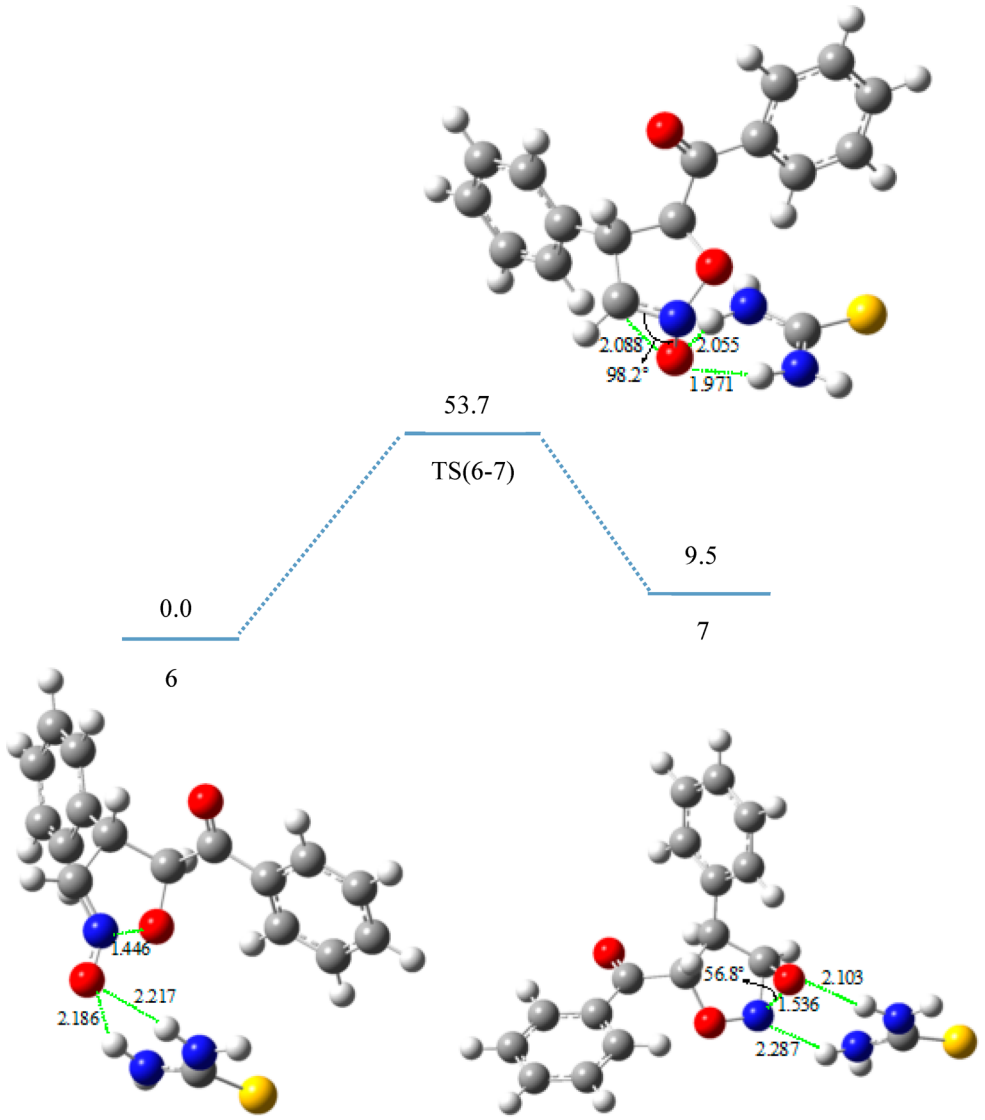

Figure 5. Relative free energies (ΔG_{298}) (in kcal/mol) of isoxazoline *N*-oxide **6** and oxaziridine **7** suggested by experimentalists with SMD solvent models at the M06-2X/6-31G(d,p) level (bond length in Å).

Table 3, and the relative energies of these two transition states are 36.4 and 32.5 kcal/mol, so that the reactions are unlikely to occur under room temperature condition. This indicates that conversion of INT2-3(B) to INT2-5(B) is not possible.

According to the result of the acid-catalyzed process, the reverse reaction barriers of INT2-3(B) and INT2-5(B) to INT1 are 35.6 and 35.8 kcal/mol for trans and 35.3 and 38.1 kcal/mol for cis conformation under the experimental conditions (room temperature and pressure). The reaction is therefore not reversible. Therefore, stereochemistry of the final product is determined after the formation of INT2-3(B) or INT2-5(B).

From Figure 5, one can see that the transition state TS(6-7) between the isoxazoline *N*-oxide **6** and oxaziridine **7** suggested by experimentalists has a barrier of about 53.7 kcal/mol calculated by M06-2X (as listed in Table 4); it is therefore impossible for the reaction to occur. This indicates that the rearrangement mechanism assumed in ref 13 is inappropriate. We therefore redesign a path where the DMAP acts as a nucleophilic catalyst and it is generated by the INT2-5(B) rearrangement reaction steps. The process is depicted in Figure 6, and the results are presented in Table 5.

The first step is the N2 of DMAP attacking the C1 of INT2-5(B) to form a new C−N bond, while the N−O bond in the original five-membered ring is disconnected to generate INT3, which is a zwitterionic intermediate. The reaction barrier of this step is 21.2 kcal/mol.

The second and third step of the reaction is a continuous proton transfer process. O1 attracts a H atom from C1 of INT3, and the reaction energy barrier is 5.3 kcal/mol. Then the H atom is moved from the O1 to O2. Reaction barrier of this step is 11.7 kcal/mol. A zwitterionic intermediate (INT5) that is more stable than INT3 is generated in this step.

The fourth step is a ring-forming reaction. O1 attacks C1 to generate a new C−O single bond. Then a four-membered ring intermediate INT6 is produced. The activation barrier is 18.0 kcal/mol.

In the fifth step, DMAP departs from INT6 to generate a more stable four-membered ring intermediate INT7. The reaction energy barrier is 5.2 kcal/mol. The fourth and fifth steps of the reaction can be considered as a intramolecular substitution reaction.

dx.doi.org/10.1021/jo4022452 | J. Org. Chem. 2013, 78, 12585−12592

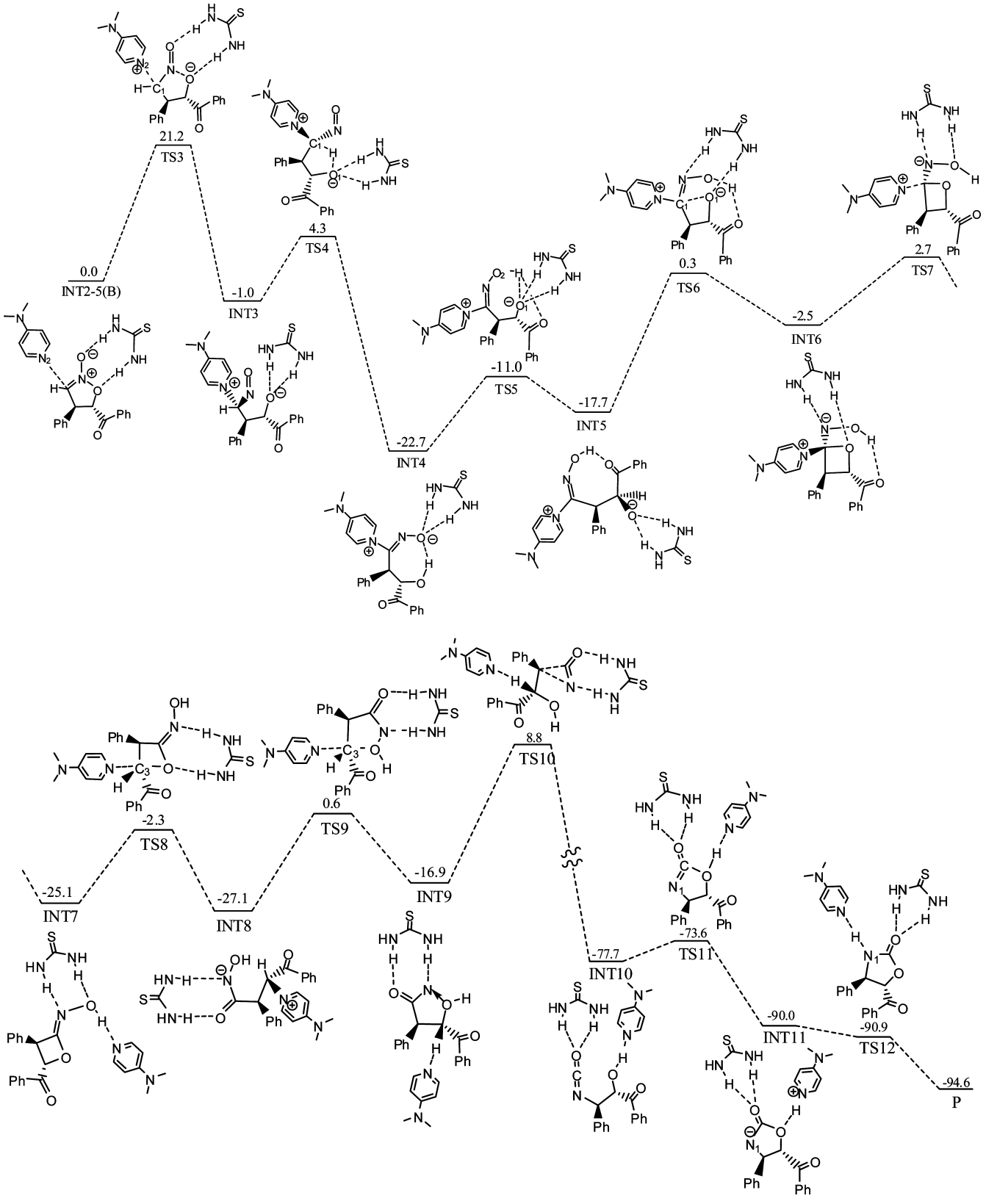

Figure 6. Relative free energies (ΔG_{298}) (in kcal/mol) of different structures in the base-catalyzed process with SMD solvent models at the M06-2X/6-31G (d,p) level.

In the sixth step, DMAP attacks C3 of INT7 again from the back of the C−O bond as a nucleophilic catalyst. The C−O bond is disconnected, and the four-membered ring is opened to regenerate the positive and negative ion intermediates INT8. In this step, the reaction energy barrier is 22.8 kcal/mol.

In the seventh step, the oxygen of OH attacks C3 and generates intermediate INT9, which has a five-membered ring

dx.doi.org/10.1021/jo4022452 | J. Org. Chem. 2013, 78, 12585−12592

structure. DMAP is released in this step, and the reaction energy barrier is 27.7 kcal/mol. The structure of INT9 (compared with INT8) is unstable and not changed after the sixth and seventh step. This is similar to the conversion process of INT2-3(B) to INT2-5(B), in which the conformation of the C3 is kept unchanged.

The eighth step is a Hofmann rearrangement[28] reaction. Isocyanate (INT10) is formed in this step. The reaction energy barrier is 25.7 kcal/mol. More details about the Hofmann rearrangement reaction will be discussed in the next section since it is the most important step.

Steps 9 and 10 of the reaction are DMAP acting as a base to transfer a proton from O1 to N1 and to produce the final product at the same time. First, DMAP takes a proton away from O1; then O1 attacks C1 to form a five-membered ring intermediate INT11. The reaction energy barrier is 4.1 kcal/mol. After that, DMAP (H+) transfers a proton to N1 again. The energy of the TS12 transition state is smaller than that of INT11. Once DMAP (H+) gets close to N1, the hydrogen atom directly transfers to N1. These two steps are very fast reactions.

In the entire base-catalyzed process, DMAP acts mostly as a nucleophilic catalyst and only once as a base. It is believed that this process is more suitably called a nucleophilic catalytic process.

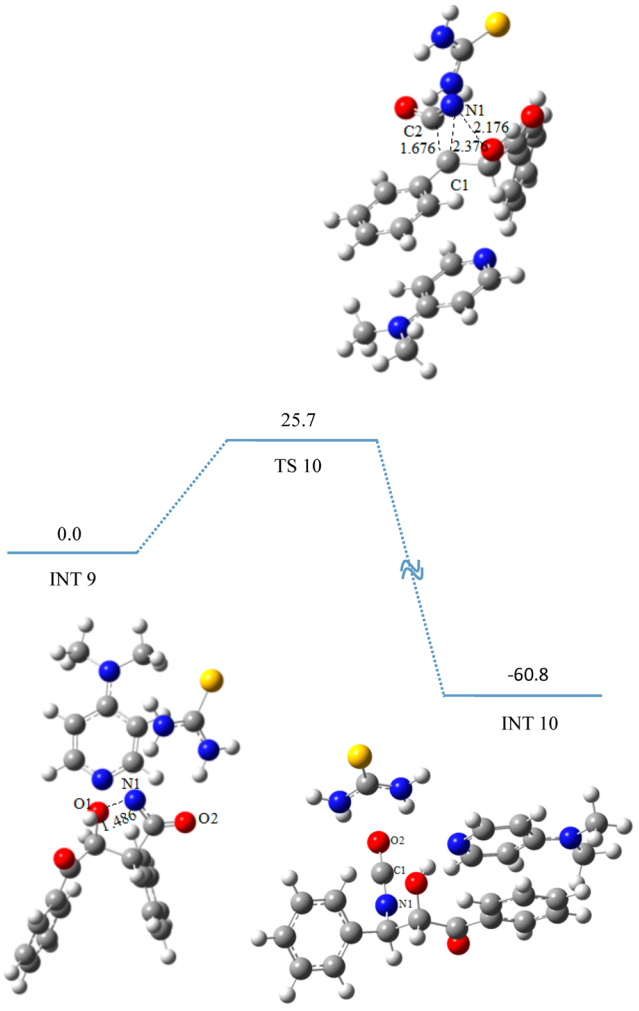

Figure 7. Relative free energies (ΔG_{298}) (in kcal/mol) of the Hofmann rearrangement reaction and the structures of INT9, TS10, and INT10 (bond length in Å).

The rearrangement mechanism presented above is more likely as the largest relative energy in step 7 is only 27.7 kcal/mol, which is much less than 53.7 kcal/mol of Xiao's proposed mechanism. Therefore, one can believe that the 10-step mechanism determined by theoretical calculations is more feasible than the one proposed by Xiao.

Hofmann Rearrangement Reaction. The Hofmann rearrangement reaction of INT9 and INT10 together with the transition state TS10 is shown in Figure 7. According to the valence bond theory, compared to INT8, INT9 is a relatively unstable intermediate because the N atom labeled as N1 in INT9 has only six outer shell electrons with a nitrene structure as shown in INT9. The oxygen atom of OH shares its lone pair electron with the nitrogen atom of INT9 to stabilize it and to form an O→N coordination bond. The bond length before the Hofmann rearrangement reaction is 1.486 Å, which is longer than a normal single O−N bond of 1.36 Å. In the transition state TS10 of the Hofmann rearrangement reaction, the O→N coordination bond is broken down with a distance between the O and N being 2.176 Å. The distance between C1 and C2 becomes 1.676 Å, and the distance of C1 and N1 is 2.376 Å. Finally, after the Hofmann rearrangement reaction, the C1−C2 and C1−N1 bonds are built. Therefore, the isocyanate INT10 is formed by the Hofmann rearrangement reaction.

Origin of the Stereoselectivity. As discussed in the base catalysis section, the chirality of the final product is determined in the acid catalysis process, in which the first additional reaction is the rate-determining step. There exist several different conformations of TS1, but we only discuss the most favorable one in energy. By inspecting and analyzing the structure of the transition state, it is found that the energy difference between TS1-trans and TS1-cis is due to the steric effect. The dihedral angle of the trans configuration of the transition state is −73.3°, while the dihedral angle of the cis one is −30.8°, with the difference between them being 42.5°.

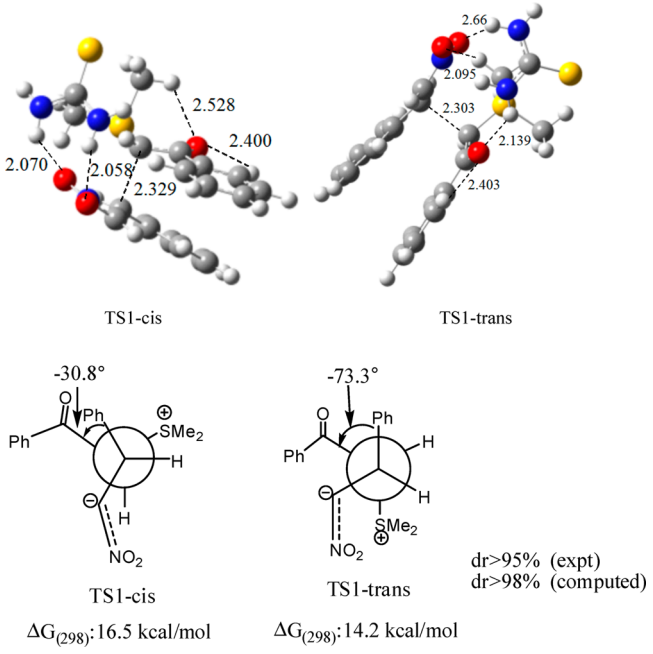

Figure 8. Structures (bond length in Å) and Newman projection types of TS1 of cis and trans configurations (relative energies are in kcal/mol).

dx.doi.org/10.1021/jo4022452 | J. Org. Chem. 2013, 78, 12585−12592

The conformation of the TS1-trans is close to the standard cross-conformation (60°), which has a lower steric energy. The conformation of the TS1-cis, however, is far away from the standard one with a difference in angle of 29.2°, which has a higher steric energy. The reason why the TS1-trans is more stable than the TS1-cis is that the distance between the positive charge center (the $-S(+)Me_2$ group) and the negative charge center (the $-NO_2$ group) is closer. Our theoretical study gives an enantiomeric excess of 98%, which is in good agreement with the value of dr (95%) in experiment (Figure 8).

CONCLUSIONS

We have performed systematic theoretical studies on the tandem reaction of sulfur ylides and nitro-olefin catalyzed by DMAP and thiourea. According to our results, we can draw the following conclusions:

(1) Addition reaction of sulfur ylides with nitro-olefin is the stereoselectivity- and rate-determining step. The stereoselectivity stems from the steric effect which results in a trans configuration dominant product. This is in good agreement with the experimental result.

(2) There are two competitive reactions in the addition reaction path. One path is to generate the nitro-cyclopropane followed by a DMAP-catalyzed rearrangement to form the isoxazoline *N*-oxide intermediate. The other path is to directly generate the isoxazoline *N*-oxide intermediate. Our calculations show that the latter is dominant.

(3) DMAP acting as both nucleophilic catalyst and base catalyst, the nitrogen oxides of isoxazoline ketone produce the final product by several processes, such as open loops, cyclizations, Hofmann rearrangement, and hydrogen migration. It is the first time that the Hofmann rearrangement involved in the cascade organocatalysis reaction is confirmed by theoretical calculations.

ASSOCIATED CONTENT

Supporting Information

Computational methods, free energies, molecular coordinates, and the B3LYP/6-31G(d,p) results. This material is available free of charge via the Internet at http://pubs.acs.org.

AUTHOR INFORMATION

Corresponding Author

*E-mail: gu@scnu.edu.cn.

Notes

The authors declare no competing financial interest.

ACKNOWLEDGMENTS

The support of the National Natural Science Foundation of China (21073067, 21273081) is greatly appreciated. The financial support from the Project Supported by Guangdong Province Universities and Colleges Pearl River Scholar Funded Scheme (2011) is also acknowledged.

REFERENCES

(1) Kakeya, H.; Morishita, M.; Koshino, H.; Morita, T.; Kobayashi, K.; Osada, H. *J. Org. Chem.* **1999**, *64*, 1052−1053.
(2) Ager, D. J.; Prakash, I.; Schaad, D. R. *Chem. Rev.* **1996**, *96*, 835−876.
(3) McManus, H. A.; Guiry, P. J. *Chem. Rev.* **2004**, *104*, 4151−4202.
(4) Desimoni, G.; Faita, G.; Joergensen, K. A. *Chem. Rev.* **2006**, *106*, 3561−3651.
(5) Mukhtar, T. A.; Gerard, D. W. *Chem. Rev.* **2005**, *105*, 529−542.
(6) Micahel, R. B.; Charles, W. F. *Angew. Chem.* **2003**, *42*, 2010−2023.
(7) Reck, F.; Zhou, F.; Girardot, M.; Kern, G.; Eyermann, C. J.; Hales, N. J.; Ramsay, R. R.; Gravestock, M. B. *J. Med. Chem.* **2005**, *48*, 499−506.
(8) Reck, F.; Zhou, F.; Eyermann, C. J.; Kern, G.; Carcanague, D.; Ioannidis, G.; Illingworth, R.; Poon, G.; Gravestock, M. B. *J. Med. Chem.* **2007**, *50*, 4868−4881.
(9) Roehrig, S.; Straub, A.; Pohlmann, J.; Lampe, T.; Pernerstorfer, J.; Schlemmer, K. H.; Reinemer, P.; Perzborn, E. *J. Med. Chem.* **2005**, *48*, 5900−5908.
(10) Kakeya, H.; Morishita, M.; Kobinata, K.; Osono, M.; Ishizuka, M.; Osada, H. *J. Antibiot.* **1998**, *51*, 1126−1128.
(11) Sekizawa, R.; Iinuma, H.; Muraoka, Y.; Naganawa, H.; Kinoshita, N.; Nakamura, H.; Hamada, M.; Takeuchi, T.; Umezawa, K. *J. Nat. Prod.* **1996**, *59*, 232−236.
(12) Grondal, C.; Jeanty, M.; Enders, D. *Nat. Chem.* **2010**, *3*, 167−178.
(13) Lu, L. Q.; Cao, Y. J.; Liu, X. P.; An, J.; Yao, C. J.; Ming, Z. H.; Xiao, W. J. *J. Am. Chem. Soc.* **2008**, *130*, 6946−6948.
(14) Lu, L. Q.; Ming, Z. H.; An, J.; Li, C.; Chen, J. R.; Xiao, W. J. *J. Org. Chem.* **2012**, *77*, 1072−1080.
(15) An, J.; Lu, L. Q.; Yang, Q. Q.; Wang, T.; Xiao, W. J. *Org. Lett.* **2013**, *15*, 542−545.
(16) Fu, G. C. *Acc. Chem. Res.* **2000**, *33*, 412−420.
(17) Xu, S. J.; Held, I.; Kempf, B.; Mayr, H.; Steglich, W.; Zipse, H. *Chem.—Eur. J.* **2005**, *11*, 4751−4757.
(18) Larionov, E.; Zipse, H.; Wiley, I. *Rev. Comput. Mol. Sci.* **2011**, *1*, 601−619.
(19) Wheeler, S. E.; McNeil, A. J.; Müller, P.; Swager, T. M.; Houk, K. N. *J. Am. Chem. Soc.* **2010**, *132*, 3304−3311.
(20) Krenske, E. H.; Houk, K. N. *Acc. Chem. Res.* **2013**, *46*, 979−989.
(21) Edward, G.; Hohenstein, S. T.; Chill, C.; David, S. *J. Chem. Theory Comput.* **2008**, *4*, 1996−2000.
(22) Zhao, Y.; Truhlar, D. G. *Theor. Chem. Acc.* **2008**, *120*, 215−241.
(23) Zhao, Y.; Truhlar, D. G. *Acc. Chem. Res.* **2008**, *41*, 157−167.
(24) Zhao, Y.; Truhlar, D. G. *Chem. Phys. Lett.* **2011**, *502*, 1−13.
(25) Becke, A. D. *J. Chem. Phys.* **1993**, *98*, 5648−5652.
(26) Cramer, C. J.; Truhlar, D. G. *Acc. Chem. Res.* **2009**, *42*, 493−497.
(27) Frisch, M. J.; Trucks, G. W.; Schlegel, H. B.; Scuseria, G. E.; Robb, M. A.; Cheeseman, J. R.; Scalmani, G.; Barone, V.; Mennucci, B.; Petersson, G. A.; Nakatsuji, H.; Caricato, M.; Li, X.; Hratchian, H. P.; Izmaylov, A. F.; Bloino, J.; Zheng, G.; Sonnenberg, J. L.; Hada, M.; Ehara, M.; Toyota, K.; Fukuda, R.; Hasegawa, J.; Ishida, M.; Nakajima, T.; Honda, Y.; Kitao, O.; Nakai, H.; Vreven, T.; Montgomery, J. A., Jr.; Peralta, J. E.; Ogliaro, F.; Bearpark, M.; Heyd, J. J.; Brothers, E.; Kudin, K. N.; Staroverov, V. N.; Kobayashi, R.; Normand, J.; Raghavachari, K.; Rendell, A.; Burant, J. C.; Iyengar, S. S.; Tomasi, J.; Cossi, M.; Rega, N.; Millam, N. J.; Klene, M.; Knox, J. E.; Cross, J. B.; Bakken, V.; Adamo, C.; Jaramillo, J.; Gomperts, R.; Stratmann, R. E.; Yazyev, O.; Austin, A. J.; Cammi, R.; Pomelli, C.; Ochterski, J. W.; Martin, R. L.; Morokuma, K.; Zakrzewski, V. G.; Voth, G. A.; Salvador, P.; Dannenberg, J. J.; Dapprich, S.; Daniels, A. D.; Farkas, Ö.; Foresman, J. B.; Ortiz, J. V.; Cioslowski, J.; Fox, D. J. *Gaussian 09*, revision B.01; Gaussian Inc.: Wallingford, CT, 2009.
(28) Dyen, M. E.; Swern, D. *Chem. Rev.* **1967**, *67*, 197.